A Hybrid Method for the study of the Mono-static Scattering from the Rough Surface and the Target Above It

R. Wang, S. R. Chai, Y. W. Wei, L. X. Guo
School of Science, Xidian University, Xi'an, China, 710071

***Abstract*-The purpose of this study is to describe a new hybrid method based on the reciprocity theorem, the physical optics (PO) and the Kirchhoff approximation (KA) for calculating the composite electromagnetic scattering from a target above a one-dimensional rough interface. The KA method is used to investigate characteristics of electromagnetic scattering from the rough interface (including the equivalent electric current densities and the scattered field from the rough interface). The scattered field from the isolated target was simulated by the PO method. Based on the reciprocity theorem, the multiple scattering up to 3rd order by the target and the underlying randomly rough interface was considered. The validity of our methods is shown by comparing our results with that of Method of Moments (MoM). It is found that our methods are in good agreement with MoM and has a higher computational efficiency.**

I. INTRODUCTION

EM scattering form a target situated above a rough surface is of great interest in recent years, with application in remote sensing, oceanic surveillance, target detecting, etc. The numerical methods such as the method of moments (MoM) [1], the finite difference time domain (FDTD) method [2], the finite element method (FEM), etc. have been developed. These techniques have a good accuracy, but their computational efficiency could not satisfy the requirement, especially when the composite scattering model is electronically large. The analytical methods and the high frequency methods, such as KA, the small perturbation method (SPM), the small slope approximation (SSA), the PO method, etc. have a high efficiency, but unable to calculate the coupling scattering field between target and rough surface. The numerical-analytical or high frequency-numerical combined methods, which includes the hybrid MoM/KA, the hybrid MoM/PO, the hybrid MoM/GTD, the hybrid FDTD/GTD, the FEM/KA [3], etc. are accurate and has high efficiency. But if the target has a complex shape or the mono-static scattering coefficient is expected, these hybrid methods are time consuming.

In this paper we discussed a new method based on reciprocity theorem, which combines KA and PO, to calculate the composite scattering from a target above a randomly rough surface.

II. SCATTERING MODELS AND FORMULATIONS

A. Scattering models

The geometric model is shown in Fig.1, a perfectly electronic conducting (PEC) target is located above 1D PEC rough interface.

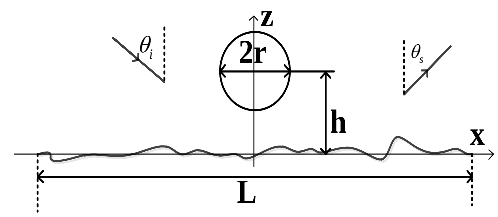

Figure 1. Geometric model of a target above 1D rough interface

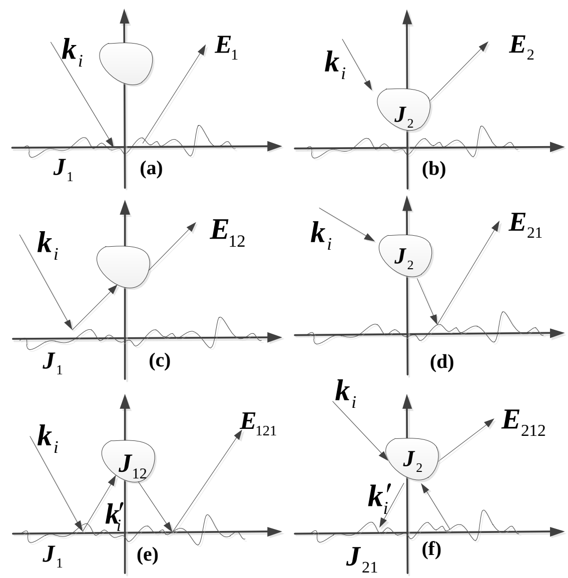

Figure 2. scattering mechanic of the composite scattering model (TE case)

Assuming that a plane wave impinging upon the model shown in Fig.1, the scattered field can be decomposed into three scattering terms: 1) direct scattered field from the rough interface $\boldsymbol{E}_1$ and from the target $\boldsymbol{E}_2$, as shown in Figure 2(a) and (b); 2) 2nd order coupling scattered field $\boldsymbol{E}_{12}$ and $\boldsymbol{E}_{21}$, as shown in Fig.2(c) and (d); 3) 3rd order coupling scattered field $\boldsymbol{E}_{121}$ and $\boldsymbol{E}_{212}$, as shown in Fig.2(e) and (f). So the total scattered field can be written as:

$$\boldsymbol{E}_{total} = \boldsymbol{E}_1 + \boldsymbol{E}_2 + \boldsymbol{E}_{12} + \boldsymbol{E}_{21} + \boldsymbol{E}_{121} + \boldsymbol{E}_{212} \tag{1}$$

In this paper, the time dependence is set to be $e^{-i\omega t}$, so, the two dimension scalar Green's function becomes

$$g(\boldsymbol{\rho}, \boldsymbol{\rho}') = \frac{i}{4} H_0^{(1)}(k|\boldsymbol{\rho} - \boldsymbol{\rho}'|) \tag{2}$$

The formula for the incident wave in our paper can be written as $\varphi_i = \exp(i\boldsymbol{k}_i \cdot \boldsymbol{\rho})$, where for TM incident wave $\boldsymbol{E}_i = \hat{y}\varphi_i$, and it is $\boldsymbol{H}_i = \hat{y}\varphi_i$ for TE polarization. $\boldsymbol{\rho} = x\hat{x} + z\hat{z}$ is the position vector where we are interested. $\boldsymbol{k}_i$ is wave-number vector of the incident wave.

B. Computation of direct scattered filed

Let incident wave illuminates on the rough interface, if the condition of validity of the standard KA is satisfied in modeling the EM scattering from the rough interface, the surface equivalent electric current density induced by the incident wave in the absence of the target can be calculated by PO, which yields:

$$\boldsymbol{J}_1(\boldsymbol{\rho}) = 2\hat{n}_s(\boldsymbol{\rho}) \times \boldsymbol{H}_i(\boldsymbol{\rho}) = \begin{cases} -\dfrac{2k}{\omega\mu}\hat{y}(\hat{n}_s \cdot \hat{k}_i)\exp(ik\boldsymbol{\rho}_s \cdot \hat{k}_i) & \text{for TE case} \\ 2\exp\left[ik\boldsymbol{\rho}_s \cdot \hat{k}_i\right]\hat{n}_s(\boldsymbol{\rho}_s) \times \hat{y} & \text{for TM case} \end{cases} \tag{3}$$

When $\boldsymbol{\rho}$ is in light region , where $\hat{n}_s$ is the unit normal vector on the rough interface , then the direct scattered field from the rough surface $\boldsymbol{E}_1$ can be given by the Huygens' Principle, the scattered electromagnetic field has forms[4] as below

$$\boldsymbol{E}_1 = i\omega\mu\int_s ds'\bar{\bar{G}}(\boldsymbol{\rho},\boldsymbol{\rho}') \cdot \boldsymbol{J}_1(\boldsymbol{\rho}') \tag{4}$$

$$\boldsymbol{H}_1 = \nabla \times \int_s ds'\bar{\bar{G}}(\boldsymbol{\rho},\boldsymbol{\rho}') \cdot \boldsymbol{J}_1(\boldsymbol{\rho}') \tag{5}$$

Where $\bar{\bar{G}}(\boldsymbol{\rho},\boldsymbol{\rho}')$ indicates dyadic Green's function, which can be written as

$$\bar{\bar{G}}(\boldsymbol{\rho},\boldsymbol{\rho}') = [\bar{\bar{I}} + \frac{1}{k^2}\nabla\nabla]g(\boldsymbol{\rho},\boldsymbol{\rho}') \tag{6}$$

Similarly, when the isolated target is illuminated by the incident wave, the direct scattered electric field has the same form with that from the rough interface:

$$\boldsymbol{E}_2 = i\omega\mu\int_s ds'\bar{\bar{G}}(\boldsymbol{\rho},\boldsymbol{\rho}') \cdot \boldsymbol{J}_2(\boldsymbol{\rho}') \tag{7}$$

$$\boldsymbol{H}_2 = \nabla \times \int_s ds'\bar{\bar{G}}(\boldsymbol{\rho},\boldsymbol{\rho}') \cdot \boldsymbol{J}_2(\boldsymbol{\rho}') \tag{8}$$

where

$$\boldsymbol{J}_2(\boldsymbol{\rho}) = 2\hat{n}_c(\boldsymbol{\rho}) \times \boldsymbol{H}_i(\boldsymbol{\rho}) = \begin{cases} -\dfrac{2k}{\omega\mu}\hat{y}(\hat{n}_c \cdot \hat{k}_i)\exp(ik\boldsymbol{\rho}_c \cdot \hat{k}_i) & \text{for TE case} \\ 2\exp\left[ik\boldsymbol{\rho}_c \cdot \hat{k}_i\right]\hat{n}_c(\boldsymbol{\rho}_c) \times \hat{y} & \text{for TM case} \end{cases} \tag{9}$$

C. Computation of 2nd order coupling scattered filed

The directed scattered field $\boldsymbol{E}_1$ and $\boldsymbol{E}_2$ can be evaluated by Huygens' Principle in (4). The challenge here is the calculation of the coupling scattered fields: $\boldsymbol{E}_{12}$, $\boldsymbol{E}_{21}$, $\boldsymbol{E}_{121}$ and $\boldsymbol{E}_{212}$. Here the reciprocity theorem was applied to solve this problem.

For TE case, according to the reciprocity theorem, consider an elementary electric current source $\boldsymbol{J}_e = \hat{y}\delta(\boldsymbol{\rho} - \boldsymbol{\rho}_0)$ placed at the observation point illuminating the target and the rough interface while the current source $\boldsymbol{J}_1$ and $\boldsymbol{J}_2$ is removed. The far-field generated by $\boldsymbol{J}_e$ is approximated as

$$\boldsymbol{E}_{ed}(\boldsymbol{\rho}) = -\hat{y}\frac{\omega\mu}{4}\sqrt{\frac{2}{\pi k\rho_0}}e^{ik\rho_0}e^{-i\pi/4}\exp(-ik\boldsymbol{\rho} \cdot \hat{k}_s) \tag{10}$$

The equivalent electric current density on the rough interface and target induced by $\boldsymbol{J}_e$ are derived as

$$\boldsymbol{J}_{e1}(\boldsymbol{\rho}_s) = 2\hat{n}_s \times \boldsymbol{H}_{ed}(\boldsymbol{\rho}_s) = 2\hat{n}_s \times \frac{\nabla \times \boldsymbol{E}_{ed}(\boldsymbol{\rho}_s)}{i\omega\mu} = -\hat{y}\frac{ik}{2}\sqrt{\frac{2}{\pi k\rho_0}}e^{-i\pi/4}e^{ik\rho_0}e^{-i\pi/2}J_{e1}^{(N)} \tag{11a}$$

$$\boldsymbol{J}_{e2}(\boldsymbol{\rho}_s) = 2\hat{n}_c \times \boldsymbol{H}_{ed}(\boldsymbol{\rho}_c) = 2\hat{n}_c \times \frac{\nabla \times \boldsymbol{E}_{ed}(\boldsymbol{\rho}_c)}{i\omega\mu} = -\hat{y}\frac{ik}{2}\sqrt{\frac{2}{\pi k\rho_0}}e^{-i\pi/4}e^{ik\rho_0}e^{-i\pi/2}J_{e2}^{(N)} \tag{11b}$$

where

$$J_{e1}^{(N)} = (\hat{n}_s \cdot \hat{k}_s)\exp(-ik\boldsymbol{\rho}_s \cdot \hat{k}_s) \tag{12a}$$

$$J_{e1}^{(N)} = (\hat{n}_s \cdot \hat{k}_s)\exp(-ik\boldsymbol{\rho}_s \cdot \hat{k}_s) \tag{12b}$$

The induced currents in the target produce an electric field on the rough interface, which can be expressed in following terms:

$$\boldsymbol{E}_{e21}(\boldsymbol{\rho}_s) = i\omega\mu\left(\bar{\bar{I}} + \frac{\nabla\nabla}{k^2}\right)\int_c \boldsymbol{J}_{e2}(\boldsymbol{\rho}_c)g(\boldsymbol{\rho}_s,\boldsymbol{\rho}_c)dc = \hat{y}\frac{k\omega\mu}{8}\sqrt{\frac{2}{\pi k\rho_0}}e^{-i\pi/4}e^{ik\rho_0}E_{e21}^{(N)} \tag{13}$$

where

$$E_{e21}^{(N)} = \int_c J_{e2}^{(N)}(\boldsymbol{\rho}_c)H_0^{(1)}(k|\boldsymbol{\rho}_s - \boldsymbol{\rho}_c|)dc \tag{14}$$

Applying the reciprocity theorem [5][6], the secondary scattered fields $\boldsymbol{E}_{12}$ (Fig.2 (c)) can be expressed as

$$\hat{y} \cdot \boldsymbol{E}_{12} = \int_s \boldsymbol{J}_1 \cdot \boldsymbol{E}_{e21}ds \tag{15}$$

Where $\boldsymbol{J}_1$ is the equivalent surface current density on the rough interface induced by the incident wave.

For the scattered field $\boldsymbol{E}_{21}$ (Fig.2 (d)), the solving process is similarly to the scattered field $\boldsymbol{E}_{12}$, which can be expressed as

$$\hat{y} \cdot \boldsymbol{E}_{21} = \int_c \boldsymbol{J}_2 \cdot \boldsymbol{E}_{e12}dc \tag{16}$$

where

$$\boldsymbol{E}_{e12}(\boldsymbol{\rho}_c) = i\omega\mu\left(\bar{\bar{I}} + \frac{\nabla\nabla}{k^2}\right)\int_s \boldsymbol{J}_{e1}(\boldsymbol{\rho}_s)g(\boldsymbol{\rho}_c,\boldsymbol{\rho}_s)ds = \hat{y}\frac{k\omega\mu}{8}\sqrt{\frac{2}{\pi k\rho_0}}e^{-i\pi/4}e^{ik\rho_0}E_{e12}^{(N)} \tag{17}$$

$$E_{e12}^{(N)} = \int_s J_{e1}^{(N)}(\boldsymbol{\rho}_s)H_0^{(1)}(k|\boldsymbol{\rho}_c - \boldsymbol{\rho}_s|)ds \tag{18}$$

For TM case, the elementary electric current source is replaced by an elementary magnetic current source $\boldsymbol{M}_e = \hat{y}\delta(\boldsymbol{\rho} - \boldsymbol{\rho}_0)$, The far-field generated by $\boldsymbol{M}_e$ is:

$$\boldsymbol{H}_{md}(\boldsymbol{\rho}) = -\hat{y}\frac{\omega\varepsilon}{4}\sqrt{\frac{2}{\pi k\rho_0}}e^{ik\rho_0}e^{-i\pi/4}\exp(-ik\boldsymbol{\rho} \cdot \hat{k}_s) \tag{19}$$

The equivalent electric current density on the rough surface induced by the elementary magnetic current source $\boldsymbol{M}_e$ is:

$$\boldsymbol{J}_{m1}(\boldsymbol{\rho}_s) = 2\hat{n}_s(\boldsymbol{\rho}_s)\times \boldsymbol{H}_{md}(\boldsymbol{\rho}_s) = -\sqrt{\frac{2}{\pi k \rho_0}}\frac{\omega\varepsilon}{2} e^{ik\rho_0} e^{-i\pi/4}\hat{n}_s(\boldsymbol{\rho}_s)\times \hat{y} J_{m1}^{(N)}(\boldsymbol{\rho}_s) \tag{20a}$$

$$\boldsymbol{J}_{m2}(\boldsymbol{\rho}_c) = 2\hat{n}_c(\boldsymbol{\rho}_c)\times \boldsymbol{H}_{md}(\boldsymbol{\rho}_c) = -\sqrt{\frac{2}{\pi k \rho_0}}\frac{\omega\varepsilon}{2} e^{ik\rho_0} e^{-i\pi/4}\hat{n}_c(\boldsymbol{\rho}_c)\times \hat{y} J_{m2}^{(N)}(\boldsymbol{\rho}_c) \tag{20b}$$

where

$$J_{m1}^{(N)}(\boldsymbol{\rho}_s) = \exp(-ik\boldsymbol{\rho}_s \cdot \hat{k}_s) \tag{21a}$$

$$J_{m2}^{(N)}(\boldsymbol{\rho}_s) = \exp(-ik\boldsymbol{\rho}_c \cdot \hat{k}_s) \tag{21b}$$

The electric field $\boldsymbol{E}_{m21}$ on the rough interface produced by $\boldsymbol{J}_{m2}$ can also be calculated by Huygens' Principle, then the secondary scattered fields in Fig.2 (c) and Fig.2 (d) becomes:

$$\hat{y}\cdot \boldsymbol{H}_{12} = -\int_s \boldsymbol{J}_1 \cdot \boldsymbol{E}_{m21} ds \tag{22}$$

$$\hat{y}\cdot \boldsymbol{H}_{21} = -\int_c \boldsymbol{J}_2 \cdot \boldsymbol{E}_{m12} dc \tag{23}$$

D. Computation of 3nd order coupling scattered filed

In order to apply reciprocity theorem for the situation shown in Fig.2 (e), $\boldsymbol{J}_{12}$ and $\boldsymbol{J}_e$ ($\boldsymbol{J}_{12}$ and $\boldsymbol{M}_e$ for TM) are treated as these two reciprocity sources, then the scattered field in this condition can be obtained as

$$\hat{y}\cdot \boldsymbol{E}_{121} = \int_c \boldsymbol{J}_{12} \cdot \boldsymbol{E}_{e12} dc \quad \text{for TE case} \tag{24}$$

$$\hat{y}\cdot \boldsymbol{H}_{121} = -\int_c \boldsymbol{J}_{12} \cdot \boldsymbol{E}_{m12} dc \quad \text{for TM case} \tag{25}$$

Using the same method we can get the scattered field of Fig.2 (f), which is [7][8]:

$$\hat{y}\cdot \boldsymbol{E}_{212} = \int_s \boldsymbol{J}_{21} \cdot \boldsymbol{E}_{e21} ds \quad \text{for TE case} \tag{26}$$

$$\hat{y}\cdot \boldsymbol{H}_{212} = -\int_s \boldsymbol{J}_{21} \cdot \boldsymbol{E}_{m21} ds \quad \text{for TM case} \tag{27}$$

where the induced equivalent electric density

$$\boldsymbol{J}_{12} = \begin{cases} \dfrac{\hat{y}k^2}{i\omega\mu}\displaystyle\int_s (\hat{n}_s\cdot\hat{k}_i)(\hat{n}_c\cdot\hat{R}_{21})\cdot\exp(ik\boldsymbol{\rho}_s\cdot\hat{k}_i)H_1^{(1)}(kR_{21})ds & \text{for TE} \\ ik\hat{n}_c\times\hat{y}\displaystyle\int_s (\hat{n}_s\cdot\hat{R}_{21})\cdot\exp(ik\boldsymbol{\rho}_s\cdot\hat{k}_i)H_1^{(1)}(kR_{21})ds & \text{for TM} \end{cases}$$

Since the length of this paper limited, some specific expressions have to be omitted.

So far, up to the directed scattered field from the target and that from the rough interface, as well as the coupling field up to 2rd and 3rd between them, the analytical expressions of normalized radar scattering cross section (NRCS) and the difference NRCS (DNRCS) can be defined as:

$$\sigma(\theta_s) = \begin{cases} 10\lg_{10}\left(\dfrac{2\pi r}{L}\left|E_{total(diff)}\right|^2\right) & \text{for TE case} \\ 10\lg_{10}\left(\dfrac{2\pi r}{L}\left|H_{total(diff)}\right|^2\right) & \text{for TM case} \end{cases} \tag{28}$$

where E_{total}, H_{total}, E_{diff} and H_{diff} are:

$$E_{total} = \hat{y}\cdot(\boldsymbol{E}_1 + \boldsymbol{E}_2 + \boldsymbol{E}_{12} + \boldsymbol{E}_{21} + \boldsymbol{E}_{121} + \boldsymbol{E}_{212}) \tag{29}$$

$$E_{diff} = \hat{y}\cdot(\boldsymbol{E}_2 + \boldsymbol{E}_{12} + \boldsymbol{E}_{21} + \boldsymbol{E}_{121} + \boldsymbol{E}_{212}) \tag{30}$$

$$H_{total} = \hat{y}\cdot(\boldsymbol{H}_1 + \boldsymbol{H}_2 + \boldsymbol{H}_{12} + \boldsymbol{H}_{21} + \boldsymbol{H}_{121} + \boldsymbol{H}_{212}) \tag{31}$$

$$H_{diff} = \hat{y}\cdot(\boldsymbol{H}_2 + \boldsymbol{H}_{12} + \boldsymbol{H}_{21} + \boldsymbol{H}_{121} + \boldsymbol{H}_{212}) \tag{32}$$

III. SIMULATION RESULTS

Fig.3-5 shows the results of the mono-static scattering from the composite model consists of a Gaussian rough surface with an infinitely cylinder above it. The incident frequency $f = 0.3\text{GHz}$, the length of rough interface is $L = 102.4\lambda$.

Fig.3 give the comparisons of our method and MoM for two different polarizations. The root mean square and correlation length of the underlying rough surface are $l = 1.5\lambda$ and $\sigma = 0.2\lambda$, respectively. The radius of infinitely cylinder is $r = 2\lambda$, the distance between the axial line of the target and the rough surface is $h = 5\lambda$.

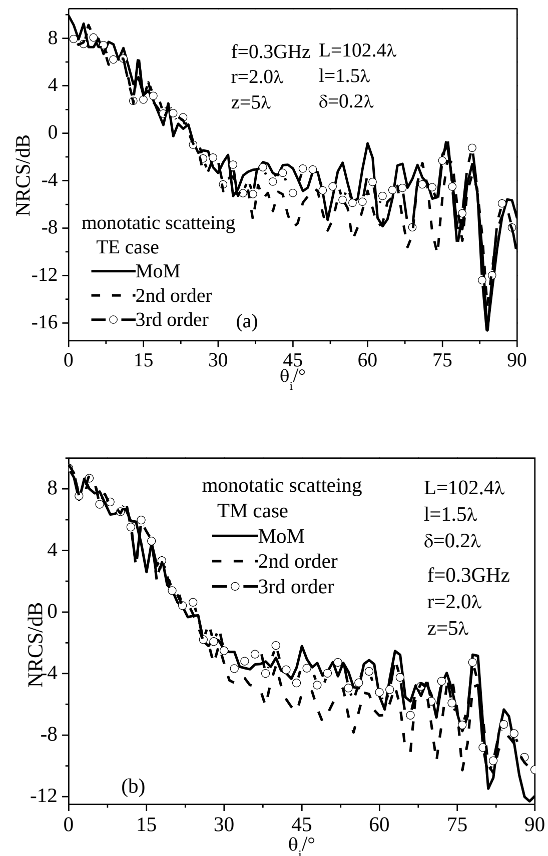

Figure 3. Comparison of the hybrid method and MoM for the mono-static scattering (a) TE case (b) TM case

From Fig.3, it is found that the mono-static NRCS of 3rd order for TM and TE by our method are in good agreement with that by MoM. Moreover, the results of 3rd order have higher accuracy than that of 2nd order. It is because the results of 3rd order take much higher coupling field between rough surface and the target into account.

Table.1 gives the simulating time of different unknowns for one same surface realization. It is obvious that our method has a higher computational efficiency than the MoM method.

TABLE.1. THE SIMULATING TIME OF DIFFERENT UNKNOWNS FOR ONE SAME SURFACE REALIZATION

Polarization of incident wave	Number of Unknowns surface+target	Time elapsed(s)	
		MoM	Our methods
TE	512+100	163	35
	1024+100	577	70
	2048+100	2138	136
TM	512+100	166	34
	1024+100	585	70
	2048+100	2151	138

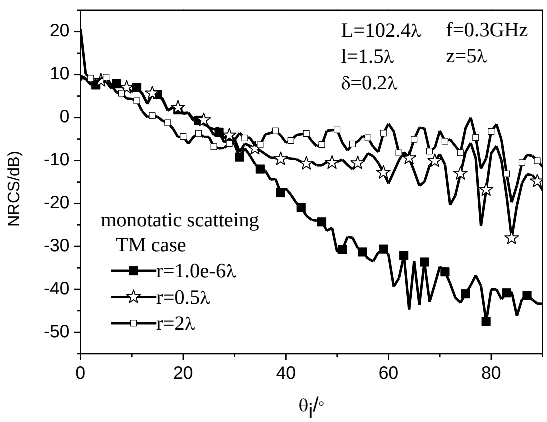

Figure 4. The mono-static scattering for different radius cylinder

Fig.4 gives the mono-static NRCS of 3rd order with different cylinder radius for TM polarization. The root mean square and correlation length of the underlying rough surface are $l = 1.5\lambda$ and $\sigma = 0.2\lambda$, respectively. The distance between the axial line of the target and the rough surface is $h = 5\lambda$. It is observed that the mono-static NRCS increases with increasing the cylinder radius. This is because that the coupling scattering becomes stronger with the large cylinder radius.

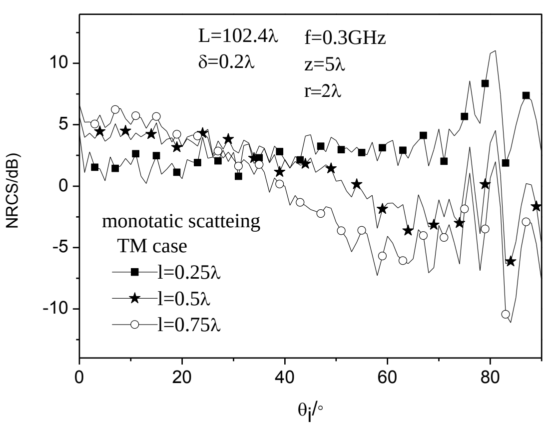

Figure 5. The mono-static scattering for different correlation length of rough surface

In Fig.5, the effect of the correlation length on the mono-static NRCS of 3rd order for TM polarization is examined. The root mean square of the rough surface and the cylinder radius are $\sigma = 0.2\lambda$ and $r = 2\lambda$, respectively. The distance between the axial line of the target and the rough surface is still $h = 5\lambda$. It is observed that the mono-static NRCS decreases over the big angular range, but increases over the small angular range with increasing l . It should be pointed out that the specular scattering becomes strong with the increasing l . For large angular, the mono-static NRCS will be weak when the results of specular scattering becomes strong. But for small angular, the results of mono-static scattering is close to that of specular scattering, so the mono-static NRCS increases with the increasing l .

IV. CONCLUSION

In this paper, an EM scattering solution for evaluating the scattering interaction between rough interface and the target is presented. The reciprocity theorem was utilized to reduce the difficulty in formulating the 2nd and 3rd order scattered fields from the composite model. The validity of this work was demonstrated by comparing the our results with that of MoM. Finally, the 3rd order coupling fields $\boldsymbol{E}_{121}$ and $\boldsymbol{E}_{212}$ ($\boldsymbol{H}_{121}$ and $\boldsymbol{H}_{212}$ for TM case) are discussed, which found that there are not reversible.

ACKNOWLEDGMENT

This work was supported by the Specialized Research Fund for the Doctoral Program of Higher Education (Grant No.20120203120023), the National Science Foundation for Distinguished Young Scholars of China (Grant No.61225002), the Postdoctoral Science Foundation of China (Grant No. 2011M501447), and the Fundamental Research Funds for the Central Universities.

REFERENCES

[1] X. Wang, C. F. Wang, and Y.B. Gan "Electromagnetic scattering from a circular target above or below rough surface," *Progress In Electromagnetics Research*, vol.40, pp. 207-227, 2003.

[2] J. Li, L. X. Guo, and H. Zeng, "FDTD investigation on the electromagnetic scattering from a target above a randomly rough sea surface," *Waves in Random and Complex Media*, vol.18, pp.641–650, 2008.

[3] J. Li, L. X. Guo, and Q. He, "Hybrid FE-BI-KA method in analyzing scattering from dielectric object above sea surface," *Electronics Letters*, vol.47 , pp. 1147–1148, 2011.

[4] Kong, J.A., *Electromagnetic Wave Theory*, John wiley & sons, 2002.

[5] R. Wang, and L. X. Guo, "Study on electromagnetic scattering from the time-varying lossy dielectric ocean and a moving conducting plate above it," *JOSA A*, vol.26, pp.517-529, 2009.

[6] T. Chiu, and K. Sarabandi, "Electromagnetic scattering interaction between a dielectric cylinder and a slightly rough surface," Antennas and Propagation, *IEEE Transactions on*, vol.47, pp.902-913, 1999.

[7] L. X. Guo, Y. H. Wang, and R. Wang, "Investigation on the electromagnetic scattering of plane wave/Gaussian beam by adjacent multi-particles," *Progress In Electromagnetics Research B*, vol.14, pp.219-245, 2009.

[8] Y. H. Wang, Y. M. Zhang, and M. H. Xia "Solution of scattering from rough surface with a 2D target above it by a hybrid method based on the reciprocity theorem and the forward–backward method," *Chinese Physics B*, vol.17, pp. 3696, 2008.